

Simulation of 1×2 OTDM router employing symmetric Mach–Zehnder switches

Z. Ghassemlooy and R. Ngah

Abstract: In high-speed all-optical time division multiplexed (OTDM) routers it is desirable to carry out data routing, switching, clock recovery and synchronisation in the optical domain in order to avoid the bottleneck due to optoelectronics conversion. The authors propose an optical switch based on all-optical symmetric Mach–Zehnder (SMZ) switching and investigate its characteristics. The proposed switch is to be used as a building block for a simple 1×2 OTDM router for asynchronous OTDM packet routing, where clock recovery, address recognition and payload routing are all carried out in the optical domain. Simulation and numerical results demonstrate that clock recovery, address recognition and payload routing are possible with small amounts of crosstalk. Also presented are simulation results for bit error rate (BER) performance for the 1×2 router. For a BER of 10^{-9} the receiver sensitivity is -26 dB compared with baseline detection without a router of -38 dB. The proposed router displays great potential for use in ultra-high-speed OTDM networks.

1 Introduction

Increasing the channel rates of lightwave networks has recently received considerable attention as a means to address the growing capacity demand in today's telecommunication systems. Optical time division multi-plexing (OTDM) technology is a promising technique to realise these ultra-high-speed optical transmission systems, and has attracted much attention because of its high capacity and great flexibility. At ultra-high speed (hundreds of gigahertz) it is desirable to carry out the entire signal routing, switching and processing in the optical domain in order to avoid bottlenecks due to the optical-to-electronic conversion. One of the key challenges in ultra-fast all-optical OTDM systems is clock recovery and subsequently synchronisation. Clock recovery and synchronisation can be achieved by sending at least one optical clock pulse with every OTDM packet. A packet is normally composed of the address bits and the payload (information bits). Multiplexing the clock pulse with the packet can be carried out in a number of ways such as: space division multiplexing, wavelength division multiplexing (WDM), orthogonal polarisation, intensity division multiplexing and time division multiplexing [1].

In space division multiplexing, the optical clock signal and the payload are carried on separate fibres. Although this scheme is the simplest to implement, there are two main drawbacks: (i) the time varying differential delay between the clock and data due to temperature variation, which may affect fibres unequally, and (ii) high installation cost. Different wavelengths are allocated to the clock and payload in the WDM scheme [2]. This technique is only practical for predetermined path lengths between nodes in single-hop networks such as point-to-point links or broad-

cast-and-select star networks. The relative delay between the clock and payload will be random in asynchronous packet-switched systems since the optical path length through which a packet travels is non-deterministic. Orthogonally polarised clock synchronisation is more suitable for small-size networks [3], whereas in larger networks correct polarisation maintenance through the network is rather difficult owing to a fibre polarization mode dispersion and other nonlinear effects. Although synchronisation based on transmission of a high intensity optical clock signal offers simplicity, maintaining the clock position and its intensity level over a long transmission span is a problem due to the impact of fibre nonlinearities [4].

Multiplexing of the clock signal in the time domain with the same intensity and wavelength as the data signal is the preferred option. At the receiver, clock extraction from the payload is carried out by employing an all-optical switching device combined with optical feedback [1]. In [1] all-optical switches based on the terahertz optical asymmetric demultiplexer (TOAD) were proposed. In the TOAD based switches, composed of a short fibre loop and a non-linear element (NLE) placed asymmetrically off the centre point of the loop, the demultiplexing operation is achieved solely by phase modulation. With the NLE located off-centre an asymmetrical switching window profile is obtained because of the counter-propagating nature of the data signals within the loop. However, placing the NLE in the centre of the fibre loop results in a double peak-switching window [5]. These characteristics of TOAD based switches result in increased crosstalk and noise. However, one might overcome these problems by employing symmetric Mach–Zehnder (SMZ) based optical switches with co-propagating signal characteristics. Recently, for the first time, we reported a 1×2 OTDM router employing SMZs with an all-optical clock recovery module [6]. A 1×2 router based on TOADs has been proposed for all-optical address recognition and single bit self-routing in a banyan-type network [7]. However, the orthogonally polarised clock signal used in the router is rather difficult to maintain due to the polarisation-mode dispersion inherent in the optical fibre link. To avoid these problems, we propose a packet

© IEE, 2005

IEE Proceedings online no. 20041017

doi:10.1049/ip-cds:20041017

Paper first received 16th January and in revised form 15th July 2004

The authors are with the School of Engineering and Technology, Northumbria University, Newcastle upon Tyne NE1 8ST, UK

E-mail: fary.ghassemlooy@unn.ac.uk

format where the clock, address and payloads all have the same intensity, polarisation, width and wavelength. In this paper, we first investigate in detail the performance of the SMZ switches and how they are used for clock recovery and routing purposes in a simple 1×2 OTDM router.

2 Nonlinear interferometer model

The SMZ interferometer consists of two arms connected to each other via two 3-dB couplers as shown in Fig. 1. Both arms of the SMZ interferometer incorporate semiconductor optical amplifiers (SOAs), positioned in the same relative location. Data and control pulses are co-propagating within the interferometer. In the absence of control signals, the SMZ is balanced in such a way that all data signals are delivered to output port 2. When control pulses are injected into the interferometer, a differential phase shift is introduced between the two arms of the interferometer thus causing the data pulses to be switched to the transmitted port (port 1).

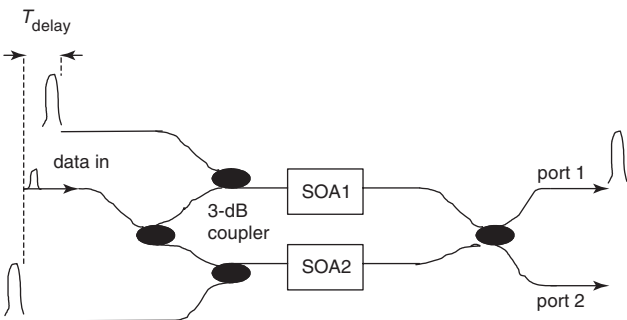


Fig. 1 SMZ configuration

The nominal switching window for the SMZ configuration in Fig. 1 is determined by the temporal delay between the control signals in both arms of the interferometer, and is given by the following interferometric equation [8]:

$$W_i(t) = 0.25\{G_1(t) + G_2(t) \pm 2\sqrt{G_1(t)G_2(t)} \cdot \cos(\Delta\phi(t))\} \quad (1)$$

where $W_i(t)$, ($i = 1$ or 2) is the SMZ switching window at the output port, G_1 and G_2 represent the temporal gain profiles of the data pulses, and $\Delta\phi$ is the phase difference between the data pulses, which is related to the gain ratio and linewidth enhancement factor κ and is given by [9]:

$$\Delta\phi = -0.5\kappa \ln(G_1/G_2) \quad (2)$$

The travelling wave semiconductor optical amplifiers (TWSOAs) have been used as NLE in the SMZ based switches, offering advantages such as: wider bandwidth, low sensitivity to the signal polarisation, larger saturated output power, tolerance to the temperature and bias current fluctuations [10]. A rate equation is usually adopted in order to assess the gain dynamics of the TWSOA. The rate equations for changes in carrier and photon densities within the active region of the device are given by [11]:

$$\frac{dN}{dt} = \frac{I}{qV} - R(N) - \frac{\Gamma \cdot g \cdot P_{av}}{A_{SOA} \cdot E_p} \quad (3)$$

$$\frac{dP_{av}}{dt} = \Gamma \cdot g \cdot P_{av} \quad (4)$$

where I is the biased current, q the electron charge, Γ the confinement factor, L_{SOA} the length of the amplifier, A_{SOA}

the active area of the SOA, E_p the photon energy, and P_{av} the average optical power over the amplifier length. g represents the differential gain of the data and control pulses, and its peak value $g_p = \alpha(N - N_o)$, which depends on the signal wavelength and the carrier density N . α is the gain coefficient and N_o the transparent carrier density. The recombination rate $R(N)$ includes the spontaneous emission and the non-radiative transitions, in particular the Auger recombination given as [11]:

$$R(N) = AN + BN^2 + CN^3 \quad (5)$$

where A is the surface and defect recombination coefficient, B the radiative recombination coefficient, C the Auger recombination coefficient, and N the carrier density.

N and P_{av} , may vary along the SOA length and are solved numerically by breaking the SOA length into a number of short length segments, as explained in detail in [5].

Solving (1) requires determination of G_1 and G_2 . The gains of the data signal at the output of the SOA1 and SOA2 at the temporal point are given respectively, as:

$$G_1(t) = \exp \left[\int_0^{L_{SOA}} \Gamma \cdot g \left(z, t + \frac{z}{V_g} \right) dz \right] \quad (6)$$

$$G_2(t) = \exp \left[\int_0^{L_{SOA}} \Gamma \cdot g \left(z, t + T_{delay} + \frac{z}{V_g} \right) dz \right] \quad (7)$$

where t is the time at which the temporal point of the data pulse enters the amplifier, T_{delay} the temporal delay between the control pulses, z/V_g the time increment in the z direction and V_g the group velocity of the control pulse.

3 Simulation and results

Two methods have been used to evaluate the SMZ switching window: a numerical model using Matlab and a simulation model using a commercial package, Virtual Photonic (VPI). The model used for the TWSOA in the numerical model is the modified version of [5] and the parameters used in the simulation are listed in Table 1 [10]. The shape of the data and control pulses are assumed to be Gaussian with a full width at half maximum (FWHM) of 2 ps. With T_{delay} equal to zero, the gain profiles of data pulses, having propagated through the SOAs, calculated from (6) and (7) are shown in Fig. 2. Since T_{delay} is zero, $G_1(t)$ and $G_2(t)$ are identical. In the absence of the control pulse a data pulse passes through the SOAs and experiences an initial gain of 20.1 dB. A high power and short duration control pulse entering the SOA produces a rapid transition in the SOAs optical properties (i.e. gain saturation). The data pulse entering the SOAs following the control pulse will experience the SOAs' pre-transition properties and as a result the gain profile drops rapidly to a value of 2.8 dB. As shown in Fig. 2, the fall time of the gain dynamics is ~ 2 ps for both SOAs, which is equivalent to the duration of the control pulses.

$G_1(t)$ and $G_2(t)$ are then substituted into (1) and (2) to obtain the SMZ switching window profile. Since the gain dynamics for both arms of the SMZ are identical then it is expected that no switching window should be observed. However, when T_{delay} is increased to 10 ps, $G_1(t)$ and $G_2(t)$ showed identical response except that $G_2(t)$ is delayed by 10 ps (Fig. 3). The SMZ symmetrical switching window with identical gain profiles and a FWHM of 10 ps is shown in the inset of Fig. 3.

Table 1: Simulation Parameters

Parameter	Value	Unit
SOA:		
Length L_{SOA}	0.3	mm
Active area A_{SOA}	3.0×10^{-13}	m^2
Transparent carrier density N_o	1.0×10^{24}	m^{-3}
Confinement factor Γ	0.15	
Differential gain g	2.78×1020	m^2
Linewidth enhancement κ	4.0	
Recombination coefficient A	1.43×10^8	1/s
Recombination coefficient B	1.0×10^{-16}	m^3/s
Recombination coefficient C	3.0×10^{-41}	m^6/s
Initial carrier density	2.8×10^{24}	m^{-3}
Total number of segments	50	
Data and control pulses:		
Wavelength of control and data pulse	1550	nm
Pulse FWHM	2	ps
Control pulse peak power	2.5	W
Data pulse peak power	2.5	μW
Data baseline bit rate	10	Gbit/s

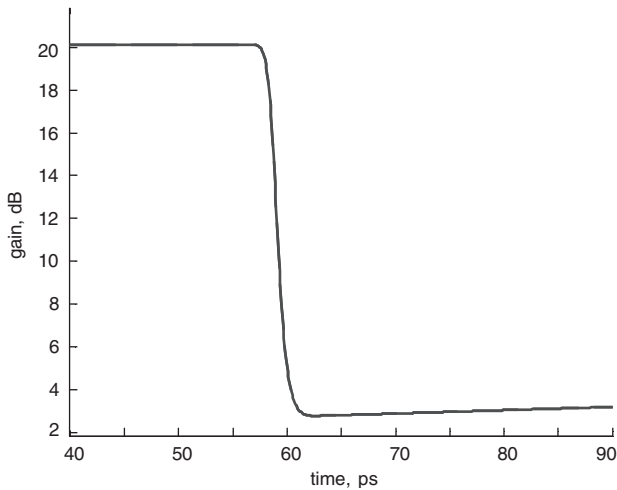


Fig. 2 Computed gain profile of data pulse propagated through SOAs with $T_{delay} = 0$

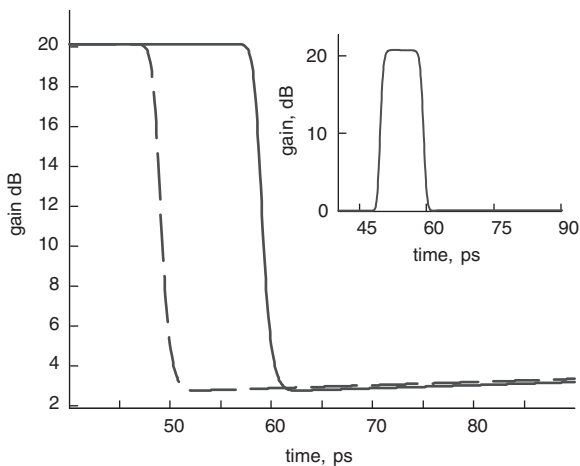


Fig. 3 Computed gain profiles of data pulse with $T_{delay} = 10$ ps
Inset: resultant SMZ switching window

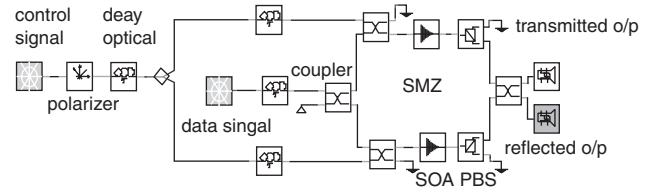


Fig. 4 VPI model of the SMZ
PBS: polarisation beam splitter

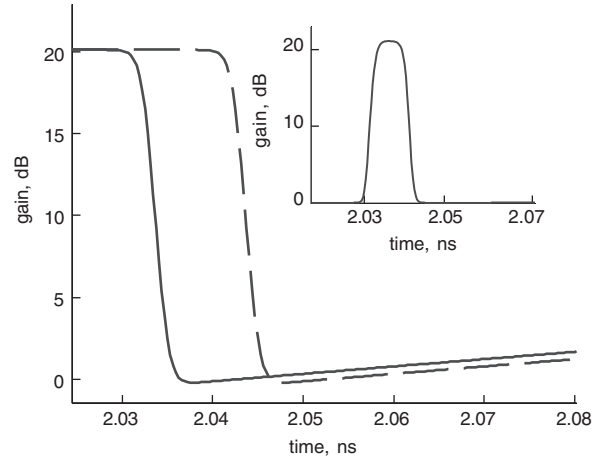


Fig. 5 Simulated gain profiles of data signals in SMZ shows inset resulting switching window

Using the same parameters as in Table 1 the proposed SMZ switch is simulated using the VPI as shown in Fig. 4. Two laser sources are used to generate the data and control pulses. The first source generates a 10 Gbit/s Gaussian shape pulse train at a wavelength of 1550 nm and a peak power of 2.5 μW , which is input to the SMZ via an optical fibre delay line (OFDL). The second source also generates a Gaussian shape pulse at 1550 nm but with a long period and a higher peak optical power of 2.5 W, which is used as the control pulse. The control pulse is passed through a 90° orthogonal polarizer to distinguish it from the data pulse since both are at the same wavelength of 1550 nm. An OFDL on each arm of the SMZ interferometer provides the required time delay T_{delay} between the two control pulses before being applied to the SMZs. An OFDL is also used for time synchronisation between the control and data pulses. All the couplers used have 50:50 splitting ratio. Figure 5 illustrates the gain profile of data pulses for the upper (solid line) and lower arms (broken line) of the SMZ. Also shown (inset) is the resulting switching window profile, which is similar to the results shown in Fig. 3. In both cases the switching windows profile is symmetrical and this is due to the co-propagation of data and control signals. The symmetrical switching window results in reduced crosstalk compared with TOAD based switches, where the switching window profile is asymmetrical.

The window amplitude increases as T_{delay} increases from zero to 4 ps and 6 ps for computed and simulated cases, respectively. No further increase in the amplitude of the transmission window is observed beyond $T_{delay} = 6$ ps, see Fig. 6. A plot of the FWHM of the switching window against T_{delay} , is shown in Fig. 7. Both simulated and computed results illustrate linear characteristics.

We next consider how a simple 1×2 OTDM router can be implemented using the proposed SMZ devices.

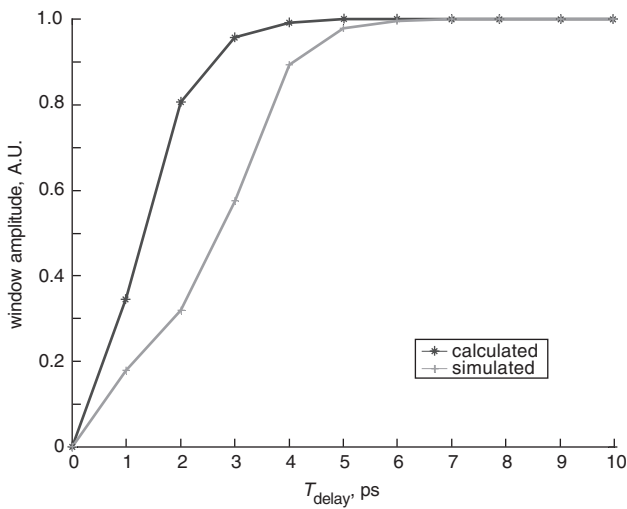


Fig. 6 Computed and simulated switching window amplitude against T_{delay}

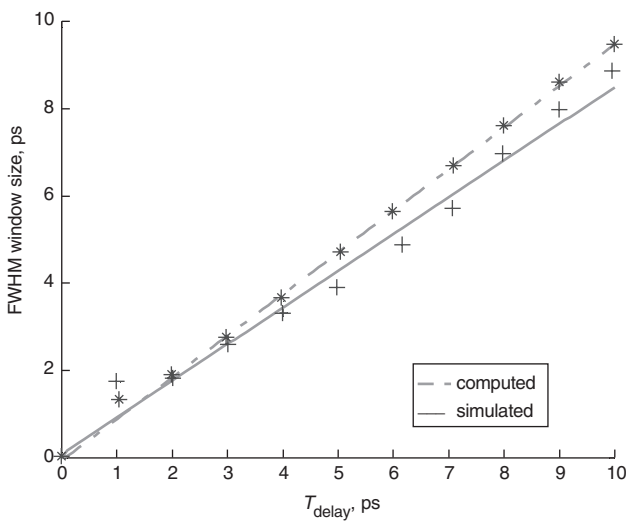


Fig. 7 Computed and simulated FWHM of switching window against T_{delay}

4 1×2 OTDM router

4.1 Self-synchronisation scheme

All-optical switches have been extensively investigated for the implementation of ultra-fast optical networks, particularly for self-synchronisation schemes [12]. In a self-synchronisation scheme, a single pulse in the first bit position of the packet, corresponding to the clock pulse, is extracted for synchronisation purposes. The clock signal could be at different wavelengths [13], polarisations [7], bit rates [14], or intensities [15] in comparison with the remaining signals within the packets. Normally a packet is composed of the clock signal, address bits and payload. In the co-propagating geometry of the SMZ, normally clock pulses have a different wavelength to that of data pulses [16, 17]. However, these schemes have a number of drawbacks: generation and transmission of packets is complicated, and the clock pulses may lose their timing relation with respect to other pulses in the same packets after propagating over a long distance [18]. To avoid these problems, we propose a packet format where the clock, the address and the payload all have the same intensity, polarisation, width and

wavelength. This is achieved by employing a highly stable single light source, such as a gain-switched distributed feedback laser (DFB) or harmonic mode-locking of erbium-doped fibre [19–21], the output of which is split into a number of channels n by a $1 \times n$ optical splitter. A number of channels dedicated to data are modulated (using external modulators) with the electrical data signals and are combined with the address and clock channels using OFDLs. The main disadvantages of the scheme are that the total transmitted power is less in comparison to the WDM scheme, which employs multiple optical generators, and the high cost of components [22].

The proposed clock and data extraction modules are shown in Fig. 8, and are composed of OFDLs, a SMZ in combination with optical feedback, a polarisation controller (PC) and a polarisation beamsplitter (PBS). The clock pulse situated at the head of the incoming OTDM packet entering the SMZ module, via an input 3-dB coupler, splits into two components with $\pi/2$ phase shift due to the input coupler, and propagate through physically separate arms of the interferometer. In the absence of the control pulse the two clock components experience the same relative phase shift during propagation, and recombine at the output 3 dB coupler before re-emerging from the reflected output port 2. The reflected clock pulse is amplified and passed through a PC before being fed back via an OFDL into the control ports of the interferometer orthogonally polarised to the data packet. OFDLs are used to introduce the delay time T_{delay} between the two input control pulses. The function of the control pulses is to change the optical properties (carrier density) of the SOAs, thus creating a switching window for extraction of the data packet (address bit and payload bit) via the transmitted output port 1 of the interferometer. At the output port 1 of the SMZ a polarisation beamsplitter has been used to separate the outgoing data and the control pulses.

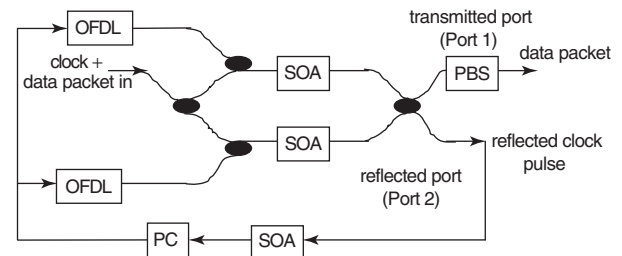


Fig. 8 Block diagram of clock extraction unit (SMZ1)

With this approach, router synchronisation is achieved by inserting only a single clock pulse, which has the same width, wavelength, polarisation and amplitude as the pulses in the payload, within the OTDM packets.

4.2 Router operation

A block diagram of the proposed 1×2 OTDM router based on three SMZ type configurations is shown in Fig. 9. The incoming OTDM packet composed of a clock pulse, an address bit and two payload bits is passed through the SMZ1 for clock extraction, as was outlined in Section 4.1. The extracted clock pulse and the address bit plus the payload from the SMZ1 are applied to the control and input ports of the SMZ2, respectively. The payload destination address bit is extracted by aligning the control pulse (i.e. the clock) with the address at the SMZ2. The

address bit of SMZ2 is fed into the control port of SMZ3 for payload routing. In a single bit routing scheme, a packet with an address bit '1' is routed to the output port 1 of SMZ3, while a packet with an address bit '0' is routed to the output port 2. Hence using this approach, photonic packets are self-routed through an all-optical ultra-fast switch without the need for optoelectronic conversion.

4.3 Simulation and results

The system shown in Fig. 9 is simulated using the VPI software shown in Fig. 10. Only a single laser source has been used in this simulation. The OTDM packet is composed of a leading clock pulse, followed by a one-bit address and two bits of payload (Fig. 11a). The bit rate chosen is 40 Gbit/s, and within each bit duration lays a pulse of very low duty cycle (8%) with an ultra-short FWHM pulsewidth of 2 ps. All the pulses within a packet have the same amplitude, width, polarisation and wavelength. A guard band of one packet duration is also used between packets.

Figure 11b shows the extracted clock pulse at the output of the SMZ1, which has the same shape as the input clock pulse except for a higher intensity, due to the SMZ switching gain of ~ 21 dB. Also shown is the channel crosstalk, which is about -37 dB (see the inset of Fig. 11b).

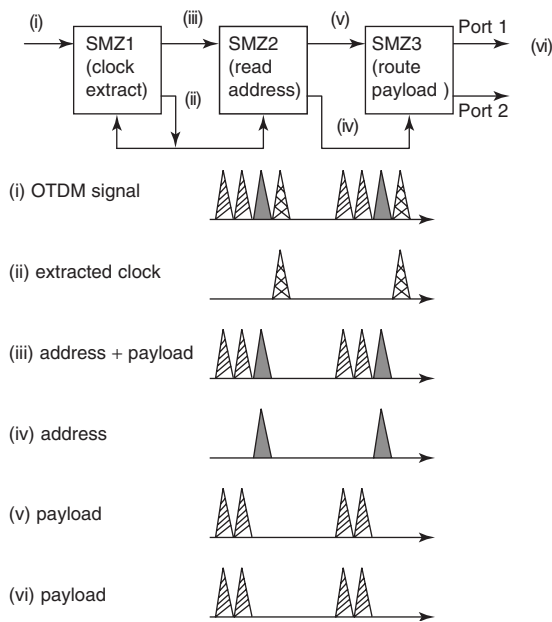


Fig. 9 Block diagram of 1×2 OTDM router and timing waveforms

This low level of channel crosstalk is mainly attributed to the symmetrical switching window profiles of the SMZs (see inset Fig. 5). Reducing the width of the switching window can reduce channel crosstalk further, however, this will result in increased relative noise intensity. The SMZ2 separates the address bit from the payload bits with the former and latter emerging from the ports 2 and 1, respectively. An address bit '1' results in routing the payloads to the output port 1 of the SMZ3, as shown in Fig. 11c.

Next we consider the bit error rate performance of the proposed router, by means of simulation. The receiver module consists of an erbium doped fibre amplifier (EDFA) and a conventional optical receiver employing a pin photodiode. The parameters used for the receiver module are shown in Table 2. The EDFA module used as an optical preamplifier is simulated using an amplification module with a wavelength-independent gain and noise figure. In order to have the same value of effective gain for both baseline detection without (back-to-back) and with the router, the gain of the EDFA is adjusted to compensate for the SMZ gain. As shown in Table 2, an EDFA gain of 25 has been used for the baseline without router. For baseline detection with the router the EDFA gain is reduced from 25 dB to 2.2 dB, making the overall gain equal to a constant value of 25 dB.

Using the parameters shown in Table 2, the BER performance for baseline detection with/without an optical router is investigated. The baseline bit rate is 10 Gbit/s and all sensitivity measures are referred to an average BER of 10^{-9} . A total of 2048 packets have been used for the BER measurement. As shown in Fig. 12, for baseline detection without an optical router, the receiver sensitivity is -38 dB. As expected the sensitivity deteriorates by almost 12 dB for the system employing an all-optical router. This increase in the power requirement is mainly due to the increase in the relative noise intensity due to the accumulation of ASE noise in the SOAs. Insets in Fig. 12 show eye diagrams of the demultiplexed channel for the baseline with and without an optical router. Notice the deterioration in the width and amplitude of the eye in the right-hand inset.

5 Conclusions

In this paper we have proposed an optical switch based on SMZs and have studied its characteristics. The proposed switch has been used as a building block for a simple 1×2 OTDM router for asynchronous packet routing. In such a router the clock recovery, address recognition and payload routing are all carried out in the optical domain. Simulation and numerical results have demonstrated that clock

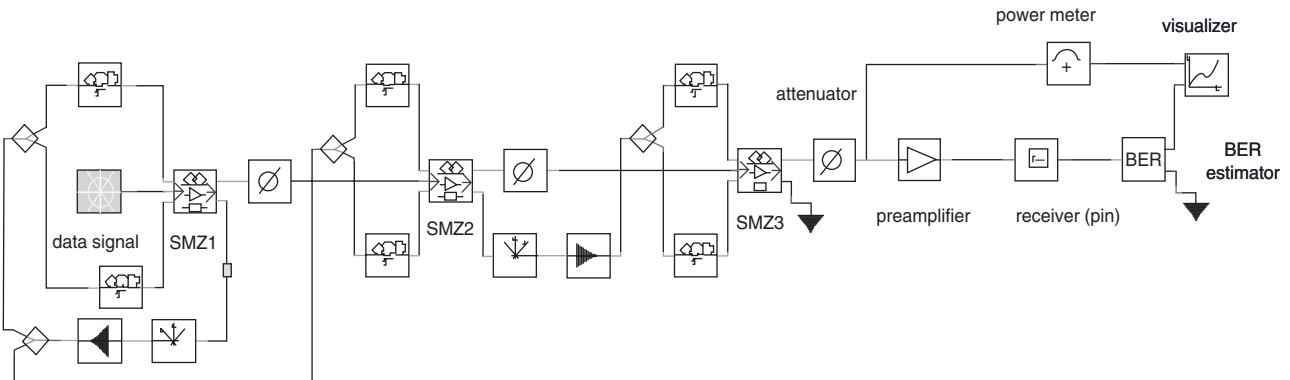


Fig. 10 Schematic block diagram of 1×2 OTDM router using VPI software

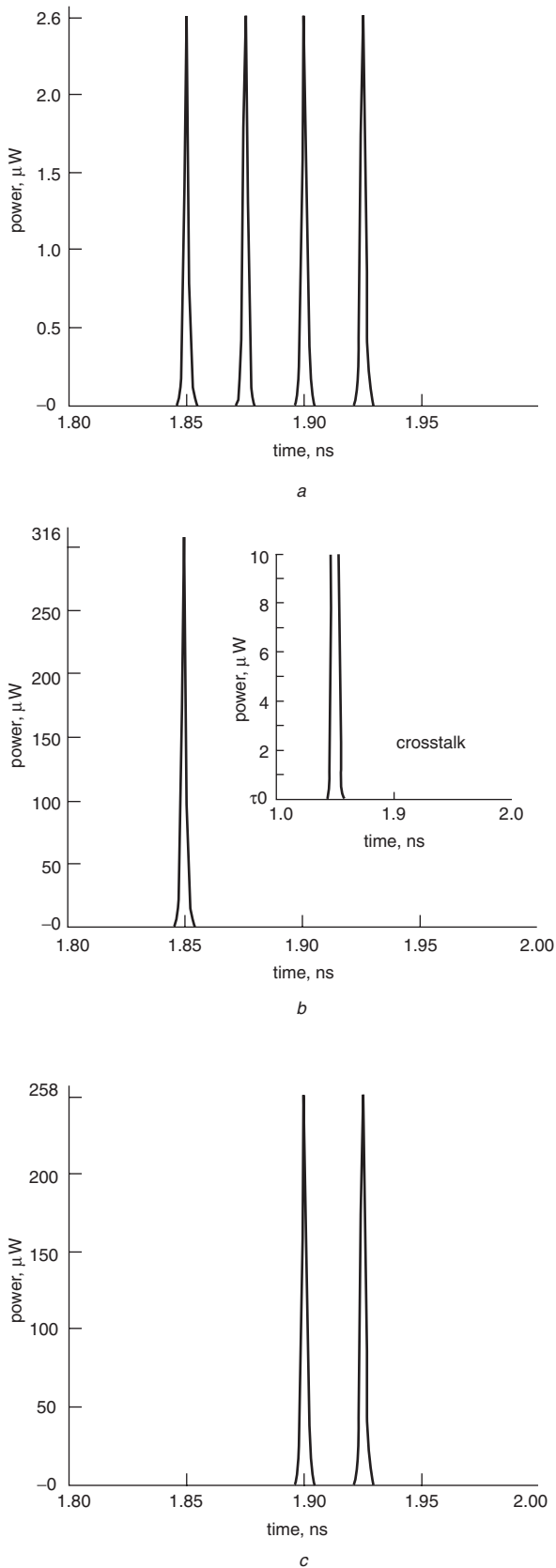


Fig. 11 Simulation results
 a Single OTDM input packet
 b Extracted clock signal at the port 2 of SMZ1 with inset showing crosstalk
 c Payload at port 1 of SMZ3

recovery, address recognition and payload routing are possible with a small amount of crosstalk. Also presented was the simulated BER performance for the 1×2 router. For a BER of 10^{-9} , the receiver sensitivity for the router

Table 2: Receiver parameters

Parameter	Value	Unit
EDFA:		
Mode	Gain controlled mode	
Noise figure	4	dB
Gain	25 (overall)	dB
Receiver		
Responsivity	1	A/W
Thermal noise	10^{-12}	A/Hz ^{1/2}
Cutoff frequency	7.0×10^9	Hz

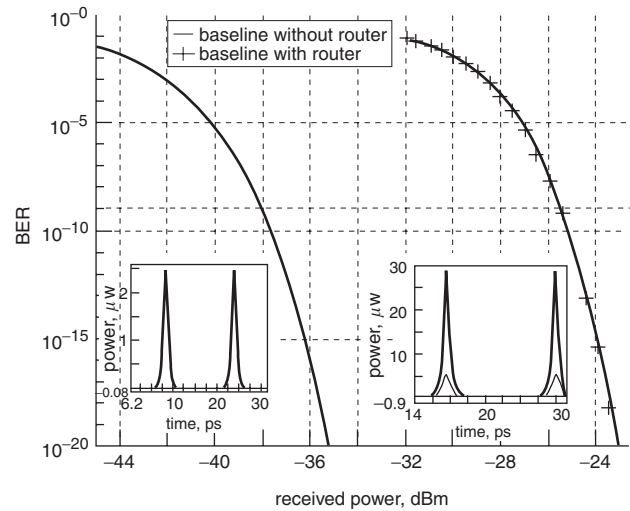


Fig. 12 BER against average received power for baseline without router, and baseline with all-optical router, and eye diagrams for baseline without router (left-hand inset) and with router (right-hand inset)

was -26 dB compared with baseline detection of -38 dB. The router proposed has great potential for ultra-high-speed OTDM networks. Further theoretical investigations of the BER and crosstalk are currently being carried out.

6 References

- Toliver, P., Glesk, I., and Prucnal, P. R.: 'All-optical clock and data separation technique for asynchronous packet-switched optical time-division-multiplexed networks', *Opt. Commun.*, 2000, **173**, pp. 101–106
- Shimazu, Y., and Tsukada, M.: 'Ultrafast photonic ATM switch with output buffers', *J. Lightwave Technol.*, 1992, **10**, pp. 265–272
- Glesk, I., Solokoff, J.P., and Prucnal, P.R.: 'All-optical address recognition and self-routing in a 250 Gbit/s packet-switched network', *Electron. Lett.*, 1994, **30**, pp. 1322–1323
- Deng, K.L., Glesk, I., Kang, K.I., and Prucnal, P.R.: 'Unbalanced TOAD for optical data and clock separation in self-clocked transparent OTDM networks', *IEEE Photonics Technol. Lett.*, 1997, **9**, pp. 830–832
- Swift, G., Ghassemlooy, Z., Ray, A. K., and Travis, J. R.: 'Modelling of semiconductor laser amplifier for the terahertz optical asymmetric demultiplexer', *IEE Proc., Circuits Devices Syst.*, 1998, **145**, (2), pp. 61–65
- Ngah, R., Ghassemlooy, Z., and Swift, G.: 'Simulation of an all optical time division multiplexing router employing symmetric Mach-Zehnder (SMZ)'. Proc. HFPSC2002, 2002, pp. 130–136
- Glesk, I., Kang, K.I., and Prucnal, P.R.: 'Demonstration of ultrafast all-optical packet routing', *Electron. Lett.*, 1997, **33**, pp. 794–795
- Schrieck, R.P., Kwakernaak, M.H., Jackel, H., and Melchior, H.: 'All-optical switching at multi-100-Gb/s data rates with Mach-Zehnder interferometer switches', *IEEE J. Quantum Electron.*, 2002, **38**, (8), pp. 1053–1061
- Eiselt, M., Pieper, W., and Weber, H.G.: 'SLALOM: semiconductor laser amplifier in a loop mirror', *J. Lightwave Technol.*, 1995, **13**, (10), pp. 2099–2112

- 10 Cheung, C.Y.: 'Noise and crosstalk analysis of all-optical time division multiplexers'. PhD Dissertation, Sheffield Hallam University, 2001
- 11 Adams, M.J., Westlake, H.J., O'Mahony, M.J., and Henning, I.D.: 'A comparison of active and passive optical bistability in semiconductors', *IEEE J. Quantum Electron.*, 1985, **QE-21**, (9), pp. 1498–1501
- 12 Tang, J.M., Spenser, P.S., Rees, P., and Shore, K.A.: 'Ultrafast optical packet switching using low optical pulse energies in a self-synchronization scheme', *J. Lightwave Technol.*, 2000, **18**, pp. 1757–1764
- 13 Shimazu, Y., and Tsuka, M.: 'Ultrafast photonic ATM switch with optical output buffers', *J. Lightwave Technol.*, 1992, **10**, pp. 265–272
- 14 Cotter, D., Lucek, J.K., Shabeer, M., Smith, K., Rogers, D.C., Nesses, D., and Cuning, P.: 'Self-routing of 100 Gbit/s packets using 6 bit 'keyword' address recognition', *Electron. Lett.*, 1995, **31**, pp. 2201–2202
- 15 Barry, R.A., Chan, V.W.S., Hall, K.L., Kintzer, E.S., Moores, J.D., Rauschenbach, K.A., Swanson, E.A., Adams, L.E., Doerr, C.R., Finn, S.G., Hauss, H.A., Ippen, E.P., Wong, W.S., and Haner, M.: 'All-optical network consortium-ultrafast TDM networks', *IEEE J. Sel. Areas Commun.*, 1996, **14**, pp. 999–1013
- 16 Nakamura, S., Ueno, Y., Tajima, K., Sasaki, T., Sugimoto, T., Kato, T., Shimoda, T., Itoh, M., Hatakeyama, H., Tamanuki, T., and Sasaki, T.: 'Demultiplexing of 168-Gbits data pulses with a hybrid-integrated symmetric Mach-Zehnder all-optical switch', *IEEE Photonics Technol. Lett.*, 2000, **12**, pp. 425–427
- 17 Diez, S., Schubert, C., Ludwig, R., Ehrke, H.J., Feiste, U., Schmidt, C., and Weber, H.G.: '160 Gbit/s all-optical demultiplexer using hybrid gain-transparent SOA Mach-Zehnder interferometer', *Electron. Lett.*, 2000, **36**, pp. 1322–1323
- 18 Xia, T.J., Kao, Y.-H., Liang, Y., Lou, J.W., Ahn, K.H., Boyraz, O., Nowak, G.A., Said, A.A., and Islam, M.N.: 'Novel self-synchronization scheme for high-speed packet TDM packet TDM networks', *IEEE Photonics Technol. Lett.*, 1999, **11**, pp. 269–271
- 19 Nakazawa, M., Suzuki, K., Yamada, E., Kubota, H., Kimura, Y., and Takaya, M.: 'Experimental demonstration of soliton data transmission over unlimited distances with soliton control in time and frequency domains', *Electron. Lett.*, 1993, **29**, pp. 729–730
- 20 Iwatsuki, K., Suzuki, K., Nishi, S., and Saruwatari, M.: '80 Gbit/s optical soliton transmission over 80 km with time/polarization division multiplexing', *IEEE Photonics Technol. Lett.*, 1993, **5**, pp. 245–248
- 21 Takada, A., and Saruwatari, M.: 'Pulse-width-tunable subpicosecond pulse generation from an actively mode-locked monolithic MQW laser electroabsorption modulator'. CLEO'94 paper CWN5, 1994
- 22 Tucker, R.S., Eisentein, G., and Korotky, S.K.: 'Optical time-division multiplexing for very high bit-rate transmission', *J. Lightwave Technol.*, 1988, **6**, pp. 1737–1749